Solvatochromic Azamethine Dyes for Probing the Polarity of Gold-Cluster-Functionalized Silica Particles

Stefan Spange,*[a] Dagmar Kunzmann,[c] Rüdiger Sens,[b] Isabelle Roth,[a] Andreas Seifert,[a] and Werner R. Thiel[d]

Abstract: Azamethine dyes of the merocyanine type [4-(*N*,*N*-di-*n*-butylamino)-2-methylphenyl]{2,4-di-keto-3-[*N*′-(*n*-hexyl)]-5-cyano-6-methyl-3-pyridinio}-1-azamethine (**1**) and [4-(*N*,*N*-diethylamino)-2-(*N*′-*tert*-butylcarboxy)-amidophenyl]-{2,4-diketo-3-[*N*′′-(*n*-hexyl)]-5-cyano-6-methyl-3-pyridinio}-1-azamethine (**2**) have been used as surface-polarity indicators for gold-cluster-functionalized silica particles. Their UV/Vis absorption maxima range from about $\lambda = 600$ to 700 nm as a function of solvent polarity and are clearly separated from the surface plasmon UV/Vis absorption band of gold ($\lambda \approx 520$–540 nm). Solvatochromism of both dyes has been investigated in 26 solvents of different polarity. The positive solvatochromic band shifts of **1** and **2** can be well expressed in terms of the empirical Kamlet–Taft solvent polarity parameters α and π^*. They are mainly sensitive to the dipolarity/polarizability (π^* term; 70–75 %) and HBD (hydrogen-bond donating) acidity (α term) of the solvent. Both dyes adsorb readily on functionalized silica samples from solutions in 1,2-dichloroethane or cyclohexane. The surface polarities of gold-cluster-functionalized silica particles, with and without co-adsorbed L-cysteine and poly(ethylenimine), have been investigated by using these solvatochromic dyes. The specific interaction of dye **2** with cysteine has been examined independently by quantum-chemical calculations by using the AM1 and PM3 methods.

Keywords: cluster compounds · cysteine · dyes/pigments · gold · silica · solvatochromism

Introduction

Silica-surface functionalization with gold clusters[1–10] was developed to chemisorb organic sulfides and disulfides selectively onto these sites for constructing patterned surfaces for biological and other applications.[1, 6, 9–11] While L-cysteine, for example, does not adsorb onto bare silica from an aqueous solution due to positive free energy of adsorption,[12] its adsorption onto gold occurs strongly with covalent metal–S bonds,[13–16] and a well-defined dimeric structure with associated carboxyl groups on the gold 110 surface results.[17] The residual silica surface is then suitable to be physically or chemically modified with other organic functionalities that do not interact with gold.[18–22] Two different environments on one surface, surface silanols and gold nanoparticles, allow the construction of tailor-made surfaces with multifunctional properties.

Gold clusters and related metal nanoparticles are characterized by their surface plasmon UV/Vis absorption band, whose position and shape depends on particle size and the polarity of the environment.[23–27] The interaction of an inorganic surface with a metal cluster or a dye is a composite of several effects. Acid–base, ion–dipole, dipole–dipole, dipole–induced dipole and dispersion forces contribute to the overall adsorption energy of a probe. Therefore, for the interpretation of a UV/Vis spectrum of any adsorbed chromophore, surface sites of different polarity as well as different contributions of specific (acid–base) and nonspecific (dipolar-polarizable) interactions must be taken into account. For this purpose, the LSER (linear solvent energy relationship) of Kamlet and Taft, which was originally developed for the quantification of intermolecular solute–solvent interactions, is well established.[28] The simplified

[a] Prof. Dr. S. Spange, Dipl.-Chem. I. Roth, Dipl.-Chem. A. Seifert
Polymer Chemistry, Institute of Chemistry
Chemnitz University of Technology, Strasse der Nationen 62
09111 Chemnitz (Germany)
Fax: (+49) 371-531-1642
E-mail: stefan.spange@chemie.tu-chemnitz.de

[b] Dr. R. Sens
BASF Aktiengesellschaft, Ludwigshafen (Germany)

[c] Dipl.-Chem. D. Kunzmann
Chair of Macromolecular Compounds
Technische Universität München
Lichtenbergstrasse 4, 85747 Garching (Germany)

[d] Prof. Dr. W. R. Thiel
Biophysical-Inorganic Chemistry, Institute of Chemistry
Chemnitz University of Technology, Strasse der Nationen 62
09111 Chemnitz (Germany)

 DOI: 10.1002/chem.200304844 © 2003 Wiley-VCH Verlag GmbH & Co. KGaA, Weinheim

Kamlet–Taft equation applied to single UV/Vis spectra of solvatochromic probe shifts is given in Equation (1):

$$\tilde{\nu} = \tilde{\nu}_o + a\alpha + b\beta + s(\pi^* + d\delta) \quad (1)$$

$\tilde{\nu}_o$ is the UV/Vis absorption maximum of the probe in a reference system, for example a nonpolar medium, α describes the HBD acidity, β the HBA (hydrogen bond accepting) ability and π^* the dipolarity/polarizability of the solvents. δ is a polarizability correction term, which is 1.0 for aromatic, 0.5 for polyhalogenated and zero for aliphatic solvents; a, b, s and d are solvent-independent correlation coefficients.[28] The original Kamlet–Taft solvent polarity parameters are averaged values derived from numerous solvent-dependent physicochemical processes.

It is expected that π^*, β and α of the oxidic component influence the surface plasmon UV/Vis band in a complex manner. Such relationships have not yet been reported.

In recent years, solvatochromic dyes have been used to study the surface polarity of functionalized silica particles and related materials in terms of empirical polarity concepts derived from solution chemistry,[29–33] for example, Reichardt's $E_T(30)$ or Kamlet and Taft's α, β and π^* scale.[34–37] Most (solvent) polarity scales are empirical and based on kinetic, thermodynamic, or spectroscopic data relating to certain reference reactions. Significantly, different empirical solvent-polarity scales correlate well with each other; this points to the existence of an underlying common feature.[39–41] Empirical solvent-polarity scales based on spectroscopic measurements usually employ changes in the UV/Vis absorption maximum of an indicator in different solvents (solvatochromism).

Classification of the polarity of metal surfaces in terms of empirical parameters is not established due to the lack of suitable probes for this purpose. An attempt to study the surface polarity of metal surfaces like gold with a solvatochromic probe was carried out by Knoll et al.[42] using a merocyanine dye. Kamat et al investigated pyrene and other fluorophores adsorbed on gold nanoparticles.[43] However, the merocyanine dye responds solely to changes of pH, and pyrene emission probably registers the surrounding environment of the gold cluster with the tenside layer and water. Adsorptions of structurally different dyes on gold and silver nanoparticles were reported by Franzen et al.[44] in order to study the effect of the dye structure on the interaction mechanism with the metal surface in relation to surface enhanced Raman scattering (SERS). The interference of electromagnetic and chemical mechanisms on the UV/Vis absorption properties of the adsorbed dyes was thoroughly discussed. However, the dyes used by Franzen are not genuine solvatochromic compounds. Their UV/Vis shifts in the adsorbed state is likely to be interfered with by weak protonation equilibria derived from citrate stabilization and other "impurities" that cannot be avoided by the preparation procedure applied. Genuine solvatochromic dyes, like Reichardt's E_T (30) or push–pull substituted aromatic compounds, show linear shifts of the position of the solvatochromic UV/Vis band as function of solvent polarity.

Unfortunately, the most commonly used solvatochromic compounds have a UV/Vis band in the region of the surface plasmon band of the metal particles that can induce electromagnetic interference. This will disturb a clean polarity measurement.

Other long-wavelength-absorbing solvatochromic dyes, such as merocyanine dyes,[45, 46] aminobenzodifuranones[47] and methine dyes,[48] have their solvatochromic UV/Vis band between $\lambda = 500$ and 600 nm. A methionine dye ($\lambda = 600$ nm) was also used to link gold nanoparticles together, but only aggregation behaviour could be detected by UV/Vis spectroscopy.[49]

In this communication, we report on two novel dyes **1** and **2**[50] as polarity probes that show solvent-induced solvatochromic bands in the visible region of the UV/Vis spectrum between about $\lambda = 600$ and 700 nm, which are clearly separated from the surface plasmon UV/Vis absorption band of gold. The dyes are also suitable for observing the surface polarity of coloured pigments such as iron oxides, organic azo-pigments and functionalized iron oxide particles.[50c] Therefore, this novel type of solvatochromic dye offers the possibility of extend the established LSE concept for silicas and synthetic polymers to coloured hybrid materials. The chemical formulae of the two dyes are presented in Scheme 1. They relate to the merocyanine type as reported in ref. [46].

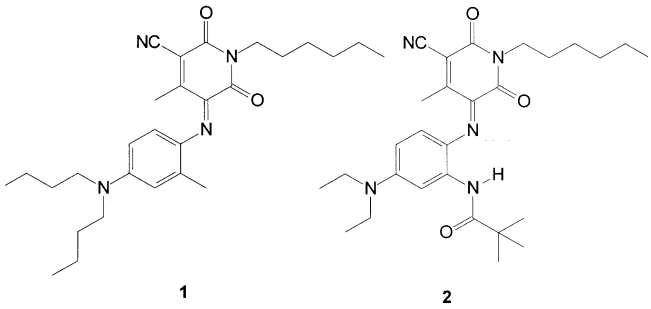

1 **2**

Scheme 1.

The solvatochromism of **1** and **2** was studied in 26 solvents in order to determine the coefficients a, b and s according to Equation (1). Adsorption on silica, amino-functionalized silica and gold-cluster-functionalized silica particles was studied, by employing the established transmission technique in organic solvents as reported.[32] The influence of the co-adsorption of L-cysteine and poly(ethylenimine) onto gold or silica on the UV/Vis absorption of **1** and **2** adsorbed onto these materials is used to observe specific adsorption effects on the surface polarity of the individual patches.

The following abbreviations are used for the functionalized silica particles in this study:

silica + H_2N-$(CH_2)_3$-$Si(OCH_3)_3$: silica–NH_2

silica–NH_2 + Au-solution : silica–$NH_2 \supset$ Au

silica–$NH_2 \supset$ Au + L-cysteine : silica–$NH_2 \supset$ Au/Cys

© 2003 Wiley-VCH Verlag GmbH & Co. KGaA, Weinheim

Results and Discussion

Solvatochromic data: The UV/Vis absorption maxima of dyes **1** and **2** in 26 solvents at room temperature and the empirical Kamlet–Taft solvent polarity parameters α, β and π^* used for the multiple square analyses are summarized in Table 1.

Table 1. UV/Vis absorption maxima of dyes **1** and **2** measured in 26 various solvents at room temperature and the empirical Kamlet–Taft solvent polarity parameters α, β and π^* of these solvents from ref. [39].

Solvent	α	β	π^*	$\tilde{\nu}_{max}10^{-3}$ [cm^{-1}] dye **1**	dye **2**
n-hexane	0.00	0.00	−0.04	16.16	15.91
p-xylene	0.00	0.12	0.43	15.85	15.67
mesitylene	0.00	0.13	0.43	16.18	15.83
cyclohexane	0.00	0.00	0.00	15.80	15.65
triethylamine	0.00	0.71	0.14	15.90	15.65
toluene	0.00	0.11	0.54	15.65	15.55
diethyl ether	0.00	0.47	0.27	15.72	15.48
CCl_4	0.00	0.10	0.28	15.55	15.38
benzene	0.00	0.10	0.59	15.46	15.36
anisole	0.00	0.32	0.73	15.36	15.22
THF	0.00	0.55	0.58	15.48	15.22
acetone	0.08	0.43	0.71	15.22	15.08
DCE[a]	0.00	0.10	0.81	15.04	14.92
CH_2Cl_2	0.13	0.10	0.82	14.97	14.88
DMF	0.00	0.69	0.88	14.99	14.88
nitromethane	0.22	0.06	0.85	14.90	14.86
n-butanol	0.84	0.84	0.47	15.06	14.86
ethanol	0.86	0.75	0.54	14.95	14.85
methanol	0.98	0.66	0.6	14.77	14.80
$CHCl_3$	0.20	0.10	0.58	14.88	14.77
benzyl alcohol	0.60	0.52	0.98	14.66	14.64
DMSO	0.00	0.76	1.00	14.73	14.71
ethan-1,2-diol	0.90	0.52	0.92	14.31	14.58
TFE[b]	1.51	0.00	0.73	14.31	14.52
HFI[c]	1.96	0.00	0.65	14.20	14.49
formamide	0.71	0.48	0.97	14.25	14.47

[a] 1,2-dichloroethane. [b] 2,2,2-trifluoroethanol. [c] 1,1,1,3,3,3-hexafluoropropan-2-ol.

Both dyes show a positive solvatochromism: increasing the solvent polarity shifts the maximum of the UV/Vis absorption band to higher wavelengths. The data range between $\lambda = 618$ (in mesitylene) and $\lambda = 704$ nm (in 1,1,1,3,3,3-hexafluoropropan-2-ol) for **1** ($\Delta\lambda = 86$ nm) and between $\lambda = 629$ (in *n*-hexane) and $\lambda = 691$ nm (in formamide) for **2** ($\Delta\lambda = 63$ nm). Thus, the dipole moment of the electronic ground state is significantly lower than that of the first excited state of the molecule. The solvatochromic UV/Vis band shifts of **1** and **2** can be expressed by means of LSERs by using the Kamlet–Taft solvent parameters.

Aromatic solvents show anomalies. Quadruple solvent–solute interactions probably contribute to the solvation of the dye in the electronic ground state; this causes an additional hypsochromic shift of the solvatochromic UV/Vis band. The following LSERs were calculated with data from Table 1.

For nonaromatic solvents:

$$\tilde{\nu}_{max}\ (\mathbf{1})\ [cm^{-1}] \times 10^{-3} = 16.01 - 0.533\alpha - 1.24\pi^*,\ (s/a = 2.26) \quad (2)$$

$n = 20$, $r = 0.976$, sd $= 0.12993$, $F < 0.0001$ ($r^2 = 0.95326$)

$$\tilde{\nu}_{max}\ (\mathbf{2})\ [cm^{-1}] \times 10^{-3} = 15.726 - 0.331\alpha - 1.002\pi^*,\ (s/a = 2.99) \quad (3)$$

$n = 20$, $r = 0.97$, sd $= 0.10181$, $F < 0.0001$ ($r^2 = 0.94103$)

Considering the solvents altogether, satisfactory multiple correlations have been calculated::

$$\tilde{\nu}_{max}\ (\mathbf{1})\ [cm^{-1}] \times 10^{-3} = 16.117 - 0.612\alpha - 1.244\pi^*;\ (s/a = 1.92) \quad (4)$$

$n = 26$, $r = 0.945$, sd $= 0.19926$, $F < 0.0001$ ($r^2 = 0.89222$)

$$\tilde{\nu}_{max}\ (\mathbf{2})\ [cm^{-1}] \times 10^{-3} = 15.830 - 0.407\alpha - 1.015\pi^*,\ (s/a = 2.33) \quad (5)$$

$n = 26$, $r = 0.924$, sd $= 0.16921$, $F < 0.0001$ ($r^2 = 0.85391$)

A typical fit is shown in Figure 1.

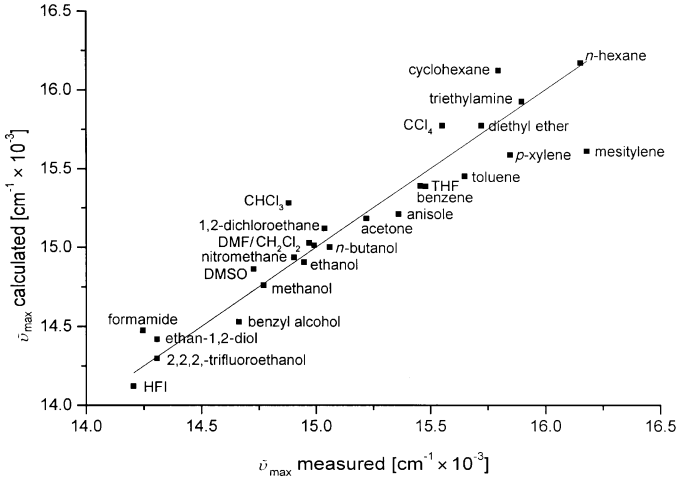

Figure 1. Calculated versus measured UV/Vis absorption maxima of dye **1** in 26 solvents.

According to Equation (1), both dyes are mainly sensitive to the π^* term of the environment, as indicated by the coefficient ratio *s*/*a*. The influence of the β term can be neglected. The solvatochromic shift range for dye **1** is slightly larger than for dye **2**. This can probably be attributed to the intramolecular H bond of the *ortho*-amide substituent to the azamethine nitrogen atom in dye **2**. The extent of the solvatochromic band shift of dye **2** reflects the influence of the π^* term, relative to the α-term, to a larger extent than dye **1** does. A similar result has been obtained for the structurally related [4-*N*,*N*-diethylamino(phenyl)]-4-*tert*-butyl-1,3-thiazol-2-[1,1-dicyanomethine]methene dye, which shows an outstanding sensitivity to π^* rather than to α.[48]

To explain the influence of the *ortho*-amido substituent, the conformational behaviour of **2** was investigated by quantum chemical calculations. Due to the size of the molecule, the semiempirical methods AM1[51] and PM3[52] implemented in the CS-MOPAC software were used. However, some additional structural restrictions had to be included in the search for geometries with minimum energies. The bulky phenyl substituent and the rigidity of the *exo* imine bond are responsible for a helical twist of the heterocyclic ring system. During the scanning of the PES for local minima, the chirality of this ring was kept untouched to prevent redundant

 © 2003 Wiley-VCH Verlag GmbH & Co. KGaA, Weinheim

calculations of enantiomers. Additionally, low-barrier rotations of certain side chains (*n*-hexyl, methyl, *tert*-butyl, NEt_2) were not included in the scanning to minimize the number of local minima. The *E* isomer of the amide group was preserved since it is favoured energetically over the *Z* isomer. As a summary of these considerations, the PES was scanned by rotation around the arrowed bonds I–III depicted in Figure 2; this resulted in 5 to 6 minimum conformations depending on the method applied. Figure 2 also shows the two

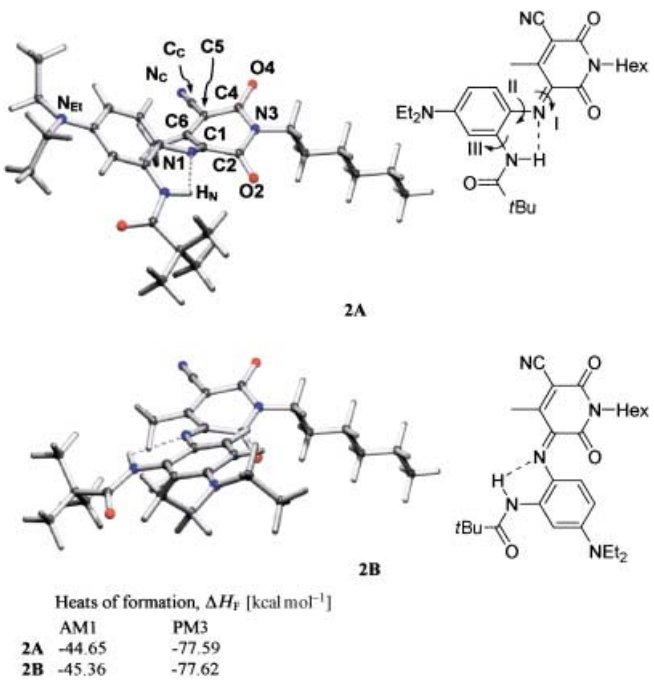

Heats of formation, ΔH_F [kcal mol^{-1}]

	AM1	PM3
2A	-44.65	-77.59
2B	-45.36	-77.62

Figure 2. Optimized geometries (AM1) of the two conformations of **2** with the lowest energies. The calculated atomic charges of marked atoms in **2A** are derived from the molecular electrostatic potential: C1 −0.13, N1 −0.39, C2 +0.54, O2 −0.44, N3 −0.39, C4 +0.68, O4 −0.45, C5 −0.56, C6 +0.15, C_{CN} +0.53, N_{CN} −0.37, N_{Et} −0.30, H_N +0.20.

conformations of dye **2** with the lowest energies, **2A** and **2B**, which were obtained with AM1 (PM3 structures are similar). Both have a weak hydrogen bond between the imine nitrogen atom and the proton of the imide group. Other local minima, which are not shown in Figure 2 were found to be just about 2–8 kcal higher in energy. The difference of the heat of formation between the two conformers **2A** and **2B** ($\Delta\Delta H_F$ = 0.71 kcal mol^{-1} (AM1) and $\Delta\Delta H_F$ = 0.03 kcal mol^{-1} (PM3)) is very small and below *RT*. The calculated dipole moment (μ in Debey, D) is slightly larger for **2B** (μ = 5.95 D (AM1) and 4.442 D (PM3)) than for **2A** (μ = 4.90 D (AM1) and 4.141 D (PM3)).

A common feature of all the optimized structures is that the imine group is only twisted by about 5°; this indicates a certain barrier to rotation for bond I. On the other hand, the barriers to rotation around bonds II and III seem to be quite low, since different rotamers of these bonds have been found in local minimum structures. The methyl group in the six position of the pyridine ring has only a sharp singlet signal at δ = 2.5 ppm in the ^{1}H NMR spectrum at 293 K. Thus, a rapidly occurring equilibrium between the two conformers takes place in solution that is fast on the NMR timescale, and an average of the two conformers is observed. Since the UV measurements with **2** were carried out in nonpolar solvents, we additionally optimized all the structures discussed here by applying a conductor-like screening model (COSMO) with a dielectric constant, ε = 1.92, typical for a nonpolar solvent. The results are in complete agreement with the data discussed above.

Adsorption on silica–NH_2 ⊃ Au particles: The degree of surface functionalization was precisely determined by quantitative elemental analysis and XPS spectroscopy (see Experimental Section).

Adsorption of colloidal gold has been carried out in aqueous solutions.[9] To keep stable conditions for the silica–NH_2 ⊃ Au particles, a residual water content on the surface could not be avoided. Thus, quantitative determination of co-adsorbed organic functionalities is difficult to determine compared with the former dried silica particles if quantitative elemental analysis has been used.

The sizes of the gold clusters have been determined to be 5 to 20 nm by electron microscopy.[53] The surface plasmon UV/Vis spectrum of the gold fraction is observed between λ = 500 and 550 nm depending on morphology and pretreatment of the silica batch used.[51]

Both dyes **1** and **2** readily adsorb on bare silica, silica–NH_2 and silica–NH_2 ⊃ Au from cyclohexane or 1,2-dichloroethane. The transparent slurries allow good quality UV/Vis transmission spectra to be taken. The results of the UV/Vis spectroscopic studies of **1** and **2** when adsorbed on the silica particles have been compiled in Table 2.

The position of the UV/Vis absorption band of **1** adsorbed on silica is comparable to that in 2,2,2-trifluoroethanol; this indicates a similar polarity. By using $\alpha \approx 1 \pm 0.1$ and $\pi^* \approx 1 \pm 0.1$, which values have been established for silica particles in 1,2-dichloroethane,[32b] then $\tilde{\nu}_{max}$ (**1**) $_{on\ silica}$ = 14240 cm^{-1} is expected from Equation (2); it was found to be 14380 cm^{-1} (Table 2). This behaviour relates well to the solvent polarity scale. In contrast, an unprecedented bathochromic shift is observed when **2** is adsorbed on bare silica particles in 1,2-dichloroethane. $\tilde{\nu}_{max}$ (**2**) $_{on\ silica}$ = 15400 cm^{-1} has been calculated from Equation (3), experimentally it is found to be 14010 cm^{-1}. The large difference between the expected and measured UV/Vis band shifts of **2** adsorbed on silica can

Table 2. UV/Vis absorption maxima of dyes **1** and **2** when adsorbed on different silicas, silica–NH_2 and silica–NH_2 ⊃ Au in 1,2-dichloroethane measured in the transmission mode.

Silica sample	Degree of functionalization [μmol m^{-2}]	$\tilde{\nu}_{max}$ 10^{-3} [cm^{-1}] dye **1**	dye **2**
KG 60	–	14.38 (15.58)[a]	14.01 (14.34)[a]
KG60–NH_2	2.38	15.58 (15.00)[a]	14.61
KG-60–NH_2 ⊃ Au	2.38	14.65 (14.70)[a]	14.44
Aerosil 380	–	14.44 (14.48)[a]	14.14 (14.15)[a]
Aerosil 380–NH_2	2	14.63 (14.91)[a]	14.61
Aerosil 380–NH_2 ⊃ Au	2	14.50 (15.08)[a]	14.55

[a] Measured by the reflectance mode after particles had been filtered, washed and dried.

© 2003 Wiley-VCH Verlag GmbH & Co. KGaA, Weinheim

probably be attributed to a specific influence of dipolar/acidic sites, because the UV/Vis shift of **2** when adsorbed on amino-functionalized silicas relates to that of **1** and does not show such additional bathochromic effect. However, either electronic or stereochemical reasons could be responsible for the observed bathochromic shift of **2**, which exceeds even the effect of the polarity of 1,1,1,3,3,3-hexafluoropropan-2-ol or formamide. We think that steric and electronic effects are associated because co-operative effects take place due to the different polar groups of dye **1** or **2**, which can interact simultaneously with two or three silanol groups. Thus, **2** can be utilized for detecting outstanding dipolar/acidic sites on a multifunctional surface.

Parameter α for bare silica is evidently larger than for silica–NH_2; this is expected and in accord with literature data.[32, 33] This is indicated by a significant hypsochromic shift of the UV/Vis band of **1** or **2** from silica to silica–NH_2. It amounts to $\Delta\lambda \approx 10$ nm. No significant differences in the UV/Vis spectra are observed when using **1** and **2** as polarity indicator between silica–NH_2 and silica–$NH_2 \supset$ Au. This is a clear indication that both dyes observe the residual silica surface and not the gold cluster sections.

The situation changes significantly when L-cysteine is co-adsorbed on silica–$NH_2 \supset$ Au. The concentration of adsorbed L-cysteine amounts to 5×10^{-5} mol g^{-1}, which corresponds well with the amount of immobilized gold cluster. Preliminary experiments (S content determination by quantitative elemental analysis) have confirmed that L-cysteine does not adsorb on bare silica from water. This was expected and is according to Basiuks studies.[12]

The UV/Vis spectra of **1** and **2** (about 10^{-4} g mol^{-1}) when adsorbed on silica, silica–$NH_2 \supset$ Au, silica–$NH_2 \supset$ Au/L-Cys and silica–$NH_2 \supset$ Au with an adsorbed poly(ethylenimine) (PEI) ($M_n = 25000$ g mol^{-1}) layer have been measured. For these studies we used silica (KG 60) $-NH_2 \supset$ Au, because silica (aerosil 300®) $-NH_2 \supset$ Au batches are aggregates consisting of Au and aerosil nano particles. Au-concentration determination was poorly reproducible for the aerosil materials.

Dye **1** is weakly sensitive to the presence of co-adsorbed L-cysteine compared with dye **2.** UV/Vis spectra of **2** adsorbed on these samples are shown in Figure 3.

A bathochromic shift of the UV/Vis absorption band of **2** takes place when L-cysteine is co-adsorbed on silica–$NH_2 \supset$ Au [$\tilde{\nu}_{max} = 14200$ cm^{-1}]; this indicates the outstanding sensitivity of **2** to dipolar/acidic surface sites. The silica–$NH_2 \supset$ Au/L-Cys site evidently shows a larger polarity than silica–$NH_2 \supset$ Au. We attribute this result to the selective adsorption of **2** on L-cysteine aggregates on the gold cluster surface.[16] In contrast, polyamine adsorption on silica–$NH_2 \supset$ Au covers the acidic surface sites;[54] this is indicated by a hypsochromic shift of **2** adsorbed on this sample [$\tilde{\nu}_{max} = 14600$ cm^{-1}].

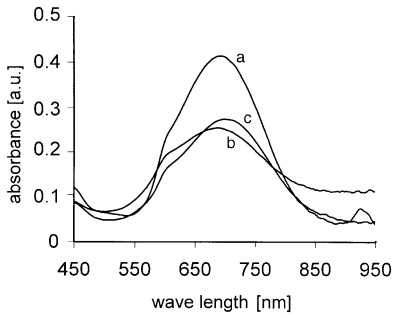

Figure 3. UV/Vis absorption spectra of dye **2** when adsorbed on a) silica–$NH_2 \supset$ Au, b) silica–$NH_2 \supset$ Au/PEI and c) silica–$NH_2 \supset$ Au/L-Cys in cyclohexane slurry. The original UV/Vis spectra of silica–$NH_2 \supset$ Au, silica–$NH_2 \supset$ Au/PEI and silica–NH_2/L-Cys, respectively, have been subtracted from those of the dye-loaded sample to avoid the disturbing shoulder of the gold plasmon resonance.

To get a deeper insight into the specific binding situation between the azamethine dye **2** and L-cysteine, we also carried out quantum-chemical calculations. In an analogous way to dye **2** (see above), L-cysteine was investigated in both the uncharged and the zwitterionic form. For the docking of the amino acid by hydrogen bonding, two possible binding sites were identified by stereoelectronic considerations (for atomic charges see legend of Figure 2): the 4-oxo site of the heterocyclic ring system, which is a structural motif of **1** too, and a hydrogen-binding triad including the 2-oxo group, the imine nitrogen atom and the proton of the amide moiety. While this triad is destroyed in structure **2B** (Figure 4), the steric restrictions for the 4-oxo site are almost the same in structures **2A** and **2B**. We therefore focused on calculating the binding of L-cysteine to **2A**.

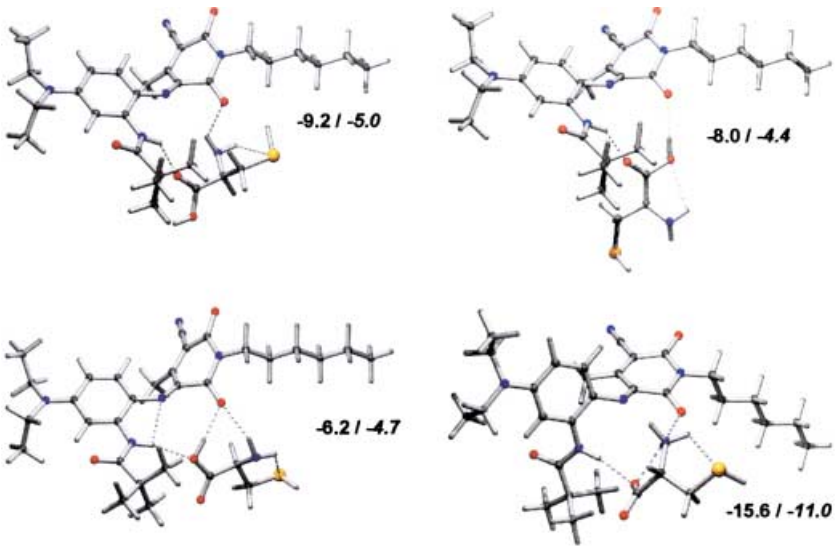

Figure 4. Optimized geometries (AM1) and binding enthalpies [kcal mol^{-1}; PM3 in italics] of three adducts of uncharged L-cysteine and one adduct of zwitterionic L-cysteine (bottom right) with **2A**.

 © 2003 Wiley-VCH Verlag GmbH & Co. KGaA, Weinheim

The uncharged form of L-cysteine [H_2N-CH(CH_2SH)-COOH] can bind to the 4-oxo site through the NH_2 protons or the proton of the carboxyl group with calculated enthalpies of about 3–6 kcal mol^{-1}. Additionally, different binding modes to the triad have been found that are energetically slightly more favourable (up to about 9 kcal mol^{-1}). The calculated thermodynamic data are in good agreement with experimental data for the hydrogen-bond strength.[55] The zwitterionic form of L-cysteine is also capable of binding to the triad ($\Delta H_{calcd} = 15.6$ kcal mol^{-1}) but a simple hydrogen bond to the 4-oxo unit could not be found. However, a combination of hydrogen bonding to O4/N_{CN} and electrostatic interaction to C6 binds the amino acid quite efficiently with a ΔH_{calcd} of about 13 kcal mol^{-1}.

The molecular structure of the azamethine dye **2** differs from its congener **1** only in the presence of the amide function in the 2-position of the benzene ring. From the results of our calculations we propose that this site, in collaboration with the azamethine nitrogen atom and the 2-oxo group of the heterocyclic ring system, is responsible for the special interaction of **2** with gold supported L-cysteine. Figure 4 shows three options for an interaction of uncharged L-cysteine and one example for an interaction of L-cysteine in its zwitterionic form with **2**.

Conclusion

Compounds **1** and **2** adsorb well onto acidic and dipolar surfaces of functionalized silicas. Their solvatochromic UV/Vis bands appear in the visible spectrum at about $\lambda = 700$ nm; this allows the investigation of coloured particles like gold-cluster-functionalized silicas without spectral interference. Small differences in the surface polarity of silica, silica–NH_2, silica–NH_2 ⊃ Au and silica–NH_2 ⊃ Au/L-Cys can be measured by dye **2**. Thus an applicable concept for determination of polarity of coloured materials has been established.

Experimental Section

Novel dyes were synthesized by an acetic anhydride-catalyzed aldol condensation from the corresponding *para*-substituted bis(*n*-alkylamino) nitrosobenzene derivative and the *N*-hexyl-3-cyano-2-hydroxy-4-methyl-6-ketopyridine according to ref. [50]. The structures of the novel dyes were confirmed ^{1}H and ^{13}C NMR spectroscopy as well as by quantitative elemental analyses.

Dye **1**: ^{1}H NMR (300 MHz, $CDCl_3$): $\delta = 1.19$ (t, CH_3), 1.48 (s, $(CH_3)_3$), 3.43 (q, -CH_2-), 6.7 and 7.47 (d, CH aromatic), 7.8 (s, -CH=); ^{13}C NMR: $\delta = 13.79$, 32.51, 39.86, 46.25, 54.10, 113.47, 115.02, 117.02, 121.18, 129.67, 136.11, 140.65, 152.48, 183.11, 191.19; elemental analysis calcd (%) for $C_{28}H_{40}N_4O_2$ (464.7): C 27.38, N 12.06, O 6.89, H 8.68; found C 27.5, N 12.2, O 7.1, H 8.6.

Dye **2**: ^{1}H NMR (300 MHz, $CDCl_3$): $\delta = 1.19$ (t, CH_3), 1.48 (s, $(CH_3)_3$), 3.43 (q, -CH_2-), 6.7 and.47 (d, CH arrogate), 7.8 (s, -CH=); ^{13}C NMR: $\delta = 13.79$, 32.51, 39.86, 46.25, 54.10, 113.47, 115.02, 117.02, 121.18, 129.67, 136.11, 140.65, 152.48, 183.11, 191.19; elemental analysis calcd (%) for $C_{28}H_{38}N_5O_3$ (493.7): C 68.13, N 14.19, O 9.72, H 7.96; found C 68.2, N 14.2, O 9.9, H 8.0.

Gold-cluster-functionalized silica particles: Gold/silica particles were synthesized by adsorption of colloidal gold solutions onto aminosilane-functionalized silica particles (silica–NH_2) according to established procedures from the literature.[7–9] The silica–NH_2 particles were also synthesized by established procedures.[18–20, 32] Surface coverage of aminosilane functionalization was calculated by Kovats' method.[56]

The gold concentration on the surface was determined by means of a calibration curve by UV/Vis spectroscopy with a stock solution of colloidal gold and presuming the difference of absorption intensity after the adsorption process to amount to the surface concentration of gold.[51] Surface gold concentrations were supported independently by XPS measurements.[57]

Physical and chemical properties of the gold-cluster-functionalized silica particles are given in the results part of this study.

UV/Vis measurements: The UV/Vis absorption maxima of the dyes **1**, **2** and **3** adsorbed on the coloured particles were recorded by using a diode-array spectrometer with glass-fibre optics. Preparation of the specific solid particles is given in the results section. A solution of the probe dye in cyclohexane or 1,2-dichloroethane (DCE) was simply added to the solid material. Care must be taken to avoid overloading the surface with the indicators used, as multilayer adsorption is expected in solution at higher concentrations or interfering absorptions from the nonadsorbed dye from the solution. Therefore, the amount of dye added was restricted to 2–3 mg of **1** or **2** per g solid, which is similar to the amount of immobilized gold. The reproducibility of the UV/Vis spectra of the adsorbed dyes was good. The mean error is less then $\lambda_{max} \pm 2$ nm and depends on residual amounts of water.

The multiple regression analyses were performed with the Microcal Origin 5.0 statistics program.

Acknowledgements

Financial support by the University of Technology, Chemnitz and the Fonds der Chemischen Industrie is gratefully acknowledged.

[1] J. P. Spatz, S. Mößmer, M. Möller, *Chem. Eur. J.* **1996**, *2*, 1552.
[2] B. Sadtler, A. Wei, *Chem. Commun*. **2002**, 1604.
[3] M. A. Zaitoun, W. R. Mason, C. T. Lin, *J. Phys. Chem. B* **2001**, *105*, 6780.
[4] Y. Jin, X. Kang, Y. Song, B. Zhang, G. Cheng, S. Dong, *Anal. Chem*. **2001**, *72*, 2843.
[5] W. Chen, W. Cai, L. Zhang, G. Wang, L. Zhang, *J. Colloid Interface Sci*. **2001**, *238*, 291.
[6] T. Ung, L. M. Liz-Marzàn, P. Mulvaney, *J. Phys. Chem. B* **2001**, *105*, 3441.
[7] T. H. Galow, A. K. Boal, V. M. Rotello, *Adv. Mater.* **2000**, *12*, 576.
[8] C. K. Yee, R. Jordan, A. Ulman, H. White, A. King, M. Rafailovitch, J. Sokolov, *Langmuir* **1999**, *15*, 3486.
[9] C. D. Keating, M. D. Musick, M. H. Keefe, M. J. Natan, *J. Chem. Educ.* **1999**, *76*, 949.
[10] S. L. Westcott, S. J. Oldenburg, T. Randall Lee, N. J. Hals, *Langmuir* **1998**, *14*, 5396.
[11] I. Willner, E. Katz, *Angew. Chem*. **2000**, *112*, 1230; *Angew. Chem. Int. Ed.* **2000**, *39*, 1180.
[12] a) V. A. Basiuk, T. V. Gromovoy, *Colloids Surf. A* **1996**, *118*, 127; b) "Thermodynamic of Adsorption of Amino Acids, Small Peptides, and Nucleic Acid Components on Silica Adsorbents", V. A. Basiuk in *Biopolymers at Interfaces* (Ed.: M. Malmsten), Surfactant Science Series 75, Marcel Dekker, New York, **1998**, p. 55.
[13] H. Grönbeck, A. Curioni, W. Andreoni, *J. Am. Chem. Soc*. **2000**, *122*, 3839.
[14] M.-Q. Xu, L. J. Wan, C. Wang, C. L. Bai, Z.-Y. Wang, T. Nozawa, *Langmuir* **2001**, *17*, 6203.
[15] S. B. Lee, C. R. Martin, *Anal. Chem*. **2001**, *73*, 768.
[16] G. Hager, A. G. Brolo, *J. Electroanal. Chem*. **2003**, published online March **2003**.
[17] A. Kühnle, T. R. Linderoth, B. Hammer, F. Besenbacher, *Nature* **2002**, *415*, 891.
[18] L. Horner, H. Ziegler, *Z. Naturforsch.* **1987**, *42b*, 643.
[19] P. M. Price, J. H. Clark, D. J. Macquarrie, *J. Chem. Soc. Dalton Trans.* **2000**, 101.
[20] R. P. W. Scott, *Silica Gel and Bonded Phases*, Wiley, **1993**.

© 2003 Wiley-VCH Verlag GmbH & Co. KGaA, Weinheim

[21] *Adsorption on Silica* (Ed.: E. Papirer), Marcel Dekker, New York **2000**.
[22] W. Godwin, R. S. Harbron, P. A. Reynolds, *Colloid Polym. Sci.* **1990**, *268*, 766.
[23] U. Kreibig, M. Vollmer, *Optical Properties of Metal Clusters*, **1995**, Springer, Berlin.
[24] C. L. Haynes, P. van Duyne, *J. Phys. Chem. B* **2001**, *105*, 5599.
[25] a) S. Link, M. A. El-Sayed, *J. Phys. Chem. B* **1999**, *103*, 8410; b) S. Link, M. B. Mohamed, M. A. El-Sayed, *J. Phys. Chem. B* **1999**, *103*, 3073.
[26] N. Toshima, *Pure Appl. Chem*. **2000**, *72*, 317.
[27] A. C. Templeton, J. J. Pietron, R. W. Murray, P. Mulvaney, *J. Phys. Chem. B* **2000**, *104*, 564.
[28] a) M. J. D. Kamlet, J.-L. M. Abboud, M. H. Abraham, R. W. Taft, *J. Org. Chem.* **1983**, *48*, 2877; b) R. W. Taft, M. J. D. Kamlet, *J. Chem. Soc. Perkin Trans. 2* **1979**, 1723.
[29] M. S. Paley, R. A. McGill, S. C. Howard, S. E. Wallace, J. M. Harris, *Macromolecules* **1990**, *23*, 4557.
[30] a) S. Spange, E. Vilsmeier, K. Fischer, S. Prause, A. Reuter, *Macromol. Rapid. Commun. (Feature)* **2000**, *21*, 643; b) S. Spange, E. Vilsmeier, Y. Zimmermann, *J. Phys. Chem. B* **2000**, *104*, 6417; c) S. Spange, Y. Zimmermann, A. Gräser, *Chem. Mater.* **1999**, *11*, 3245; d) Y. Zimmermann, S. Spange, *New. J. Chem.* **2002**, *26*, 1179.
[31] S. Spange, C. Schmidt, H. R. Kricheldorf, *Langmuir* **2001**, *17*, 856.
[32] a) S. Spange, A. Reuter, W. Linert, *Langmuir* **1998**, *14*, 3479; b) S. Spange, A. Reuter, *Langmuir* **1999**, *15*, 141; c) S. Spange, A. Reuter, D. Lubda, *Langmuir* **1999**, *15*, 2103; d) S. Spange, A. Reuter, S. Prause, C. Bellmann, *J. Adhes. Sci. Technol.* **2000**, *14*, 399.
[33] D. J. Macquarrie, S. J. Tavener, G. W. Gray, P. A. Heath, J. S. Rafelt, S. I. Saulzet, J. J. E. Hardy, J. H. Clark, P. Sutra, D. Brunel, F. di Renzo, F. Fajula, *New. J. Chem.* **1999**, *23*, 725.
[34] a) C. Reichardt, *Solvents and Solvent Effects in Organic Chemistry*, 2nd ed., VCH, Weinheim, **1988**, and references therein; b) C. Reichardt, *Chem. Rev.* **1994**, *94*, 2319.
[35] V. Gutmann, *Coord. Chem. Rev.* **1976**, *18*, 225.
[36] W. Liptay, *Z. Naturforsch.* **1965**, *20a*, 1441.
[37] P. Suppan, *J. Photochem. Photobiol. A* **1990**, *50*, 293.
[38] S. Nigam, S. Rutan, *J. Appl. Spectrosc*. **2001**, *55*, 362A.
[39] Y. Marcus, *Chem. Soc. Rev.* **1993**, 409.
[40] L. P. Novaki, O. A. El Seoud, *Ber. Bunsen-ges.* **1996**, *100*, 648.
[41] N. Palm, V. Palm, *Org. React. (Tartu)* **1997**, *104*, 141.
[42] K. Fujita, M. Hara, H. Sasabe, W. Knoll, *Langmuir* **1998**, *14*, 7456.
[43] a) G. K. Thomas, P. V. Kamat, *J. Am. Chem. Soc*. **2000**, *122*, 2655; b) P. V. Kamat, *J. Phys. Chem. B* **2002**, *106*, and references therein.
[44] S. Franzen, J. C. W. Folmer, W. R. Glomm, R. O'Neal, *J. Phys. Chem. A* **2002**, *106*, 6533.
[45] L. G. S. Brooker, A. C. Craig, D. W. Hesseltine, P. W.Jenkins, L. L.Lincoln, *J. Am. Chem. Soc*. **1965**, *87*, 2443.
[46] a) F. Würthner, S. Yao, J. Schilling, R. Wortmann, M. Redi-Abstriro, E. Mecher, F. Gallego-Goméz, *J. Am. Chem. Soc*. **2001**, *123*, 2810; b) F. Würthner, R. Wortmann, K. Meerholz, *Chem. Phys. Chem.* **2002**, *3*, 17.
[47] A. A. Gorman, M. G. Hutchings, P. D. Wood, *J. Am. Chem. Soc*. **1996**, *118*, 8497.
[48] S. Spange, R. Sens, Y. Zimmermann, A. Seifert, I. Roth, S. Anders, K. Hofmann, *New J. Chem*. **2003**, *27*, 520.
[49] W. Cheng, J. Jiang, S. Dong, E. Wang, *Chem. Commun*. **2002**, 1706.
[50] a) R. Sens, A. J. Schmidt, S. Beckmann, K.-H. Etzbach, **1997**, **EP** 0 791 035 B1, BASF AG (DE); b) R. Sens, S. Beckmann, K.-H. Etzbach, A. J. Schmidt, **1998**, US Patent 5811370, BASF AG (DE); c) S. Spange, R. Sens, A. Seifert, S. Wolf, unpublished results.
[51] a) M. Dewar, W. Thiel, *J. Am. Chem. Soc.* **1977**, *99*, 4499; b) M. J. S. Dewar, M. L. McKee, H. S. Rzepa, *J. Am. Chem. Soc.* **1978**, *100*, 3607; c) M. J. S. Dewar, E. G. Zoebisch, E. F. Healy, *J. Am. Chem. Soc.* **1985**, *107*, 3902; d) M. J. S. Dewar, C. H. Reynolds, *J. Comp. Chem.* **1986**, *2*, 140.
[52] a) J. J. P. Stewart, *J. Comp. Chem.* **1989**, *10*, 209; b) J. J. P. Stewart, *J. Comp. Chem.* **1989**, *10*, 221.
[53] D. Kunzmann, *Diploma Thesis* **2000**, Chemnitz University of Technology, (Germany).
[54] I. Voigt, F. Simon, K. Estel, S. Spange, *Langmuir* **2001**, *17*, 3080.
[55] T. Steiner, *Angew. Chem.* **2002**, *114*, 50; *Angew. Chem. Int. Ed.* **2002**, *41*, 48.
[56] E. Kovàts, *Adv. Coll. Sci*. **1976**, *6*, 95.
[57] F. Simon, D. Kunzmann, S. Spange, unpublished results.

Received: February 12, 2003 [F4844]

 © 2003 Wiley-VCH Verlag GmbH & Co. KGaA, Weinheim